JME

Journal of Mining & Environment,
Vol.6, No.1, 2015, 55-62.

Underground contour (UGC) mapping using potential field, well log and comparing with seismic interpretation in Lavarestan area

M. Fakhrerad[1], A. Nejati Kalateh[1*] and Sh. Ghomi[2]

1. School of Mining, Petroleum & Geophysics Engineering, University of Shahrood, Shahrood, Iran
2. MSc in Geophysics, National Iranian Oil Company Exploration Directorate

Received 14 September 2013; received in revised form 9 October 2014; accepted 19 October 2014
**Corresponding author: nejati@shahroodut.ac.ir (A. Nejati Kalateh).*

Abstract

Coastal Fars gravimetry project in Fars province was carried out to find the buried salt domes and to determine characteristics of faults in this area. The Lavarestan structure was covered by 4203 gravimetry stations in a regular grid of 1000*250 m. Depth structural model of this anticline made in previous studies was based on geological evidences and structural geology measurements. In order to have a complete coverage of Lavarestan anticline, 4 profiles with appropriate intervals were selected on gravity data for further processing and interpretation. 2D inverse modeling was performed on these profiles using Encome Modelvision and Encome PA software. Geometrical and physical parameters of each layer were changed step by step and forward gravity calculations were repeated until we reached a desirable fitting between observed and calculated gravity anomaly. The results of 2D gravity modeling were focused on Lower Paleozoic and Kazerun (cap rock) top horizon, also the underground contour map was extracted from seismic data after interpretation. The results show appropriate correlation between the underground contour map of 2D gravity modeling and interpretation of seismic data.

Keywords: *Inverse Modelling, Potential Field Data, Underground Contour Map, Encome Modelvision, Lavarestan.*

1. Introduction

Exploration of structural oil traps (anticline and salt plug) is an important objective of the interpretation of gravity data. Potential field methods, in particular gravity technique have an important role in detecting subsurface geological structures including oil traps. An identified gravity anomaly could be caused by a number of possible mass bodies with different dimensions [1]. According to Lowrie [2], large scale deep-seated geological structures cause broad and low amplitude regional anomalies in the gravitational field while shorter wavelength residual anomalies are due to shallow structures. Removal of regional effects from the measured gravity data causes residual anomaly. The use of appropriate anomaly separation filters strongly influences the data interpretation and provides useful information to detect subsurface oil trap. Modelling as the final stage in gravity interpretation is conducted on the residual gravity map in which long-wavelength regional effects are efficiently removed from the gravity data; taking geological and depth control information from well logs or seismic data into consideration [3].

Jenkins et al. [4] presented a method for gravity modeling of salt domes and pinnacle reefs. They supposed that, the density contrast between the host rocks varied with the radius of a cylindrically symmetric body and depth. In this method, the density function was interpolated from data points by the use of a piecewise continuous cubic polynomial basis function. Talwani [5] presented a method for robust non-linear inversion of gravity gradients. He provided several synthetic examples together with a field example of inversion. Oruc [6] presented the application of the tilt angle map (TAM) obtained from the first vertical gradient of a gravity anomaly for edge detection and depth estimation of geological structures. Barnes and Barraud [7] developed a spatially based surface inversion algorithm to solve geometric interface between geologic bodies.

Gravimetrical surveying of coastal Fars was performed by NIOC in 4203 stations along with 44 profiles in order to determine the Lavarestan anticline [8]. In the present work, attention has been focussed on Depth structural model of this anticline, based on geological evidences and surface geological measurements. To achieve the goal, commercial computer-based softwares called Encome ModelVison Pro. and Encome PA Pro. [9] were used to present 2D modeling and underground contour maps to evaluate the conformity between gravity and seismic data. Before modelling, the regional effects were removed from the Bouguer values and an appropriate residual gravity map was produced.

2. Geographical and geological location

Lavarestan anticline is located in southeast part of Zagros faulted belt and in structural state of coastal Fars, which has a total area of 450 km^2. Average elevation of this region is 1050 m [10]. Lavarestan anticline is limited to Dehno anticline and Hendurabi fault from west, to salt domes from east, to Gezeh anticline from north and to Khalfani anticline and northern shores of Persian Gulf from south. Figure 1 shows the location of survey area.

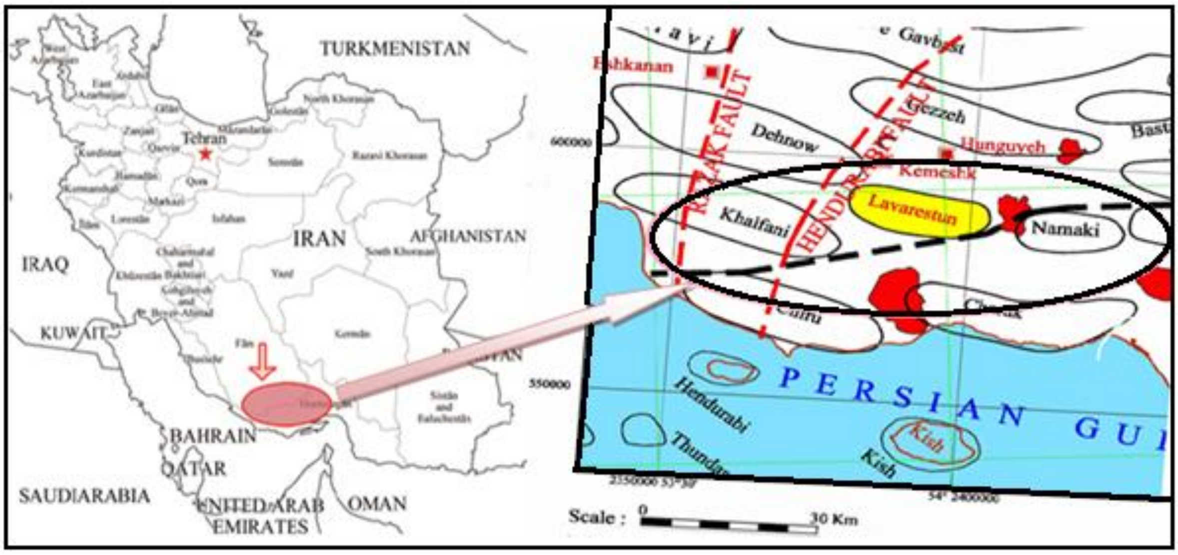

Figure 1. Location of survey area.

General strike of this anticline is northwest to southeast and actually very close to east-west direction. Except for the mentioned salt domes in east, the oldest structures in this anticline are traced back to Cretaceous, and all structure outcrops have an age of Cretaceous to Quaternary. These sediments include Gurpi, Pabdeh, Asmari, Gachsaran, Fars group and Bakhtiari formation and modern era sediments [11]. The appropriate reservoir rock, based on NIOC reports, is the Kangan formation from Dehram group while Dashtak formation from Kazerun group is the cap rock [10].

3. Background of geophysical modeling

Regardless of which system is used (2D or 3D), there are two main modeling methods: inverse and forward modeling. The former has two sub-models: parametric and smooth modeling. In this study, parametric inverse modeling was performed using Encome Modelvision pro software. In this method, geometrical and physical parameters are changed step by step and calculations will be repeated until differences between observed and calculated anomaly is minimized.

Although the potential field depends nonlinearly on certain source parameters, this dependency is nearly linear with respect to sufficient changes in those parameters. For example, the gravity field due to a set of polygonal prisms can be expanded in Taylor's series based on changes in the positions of the coordinates of the polygons. If changes in coordinates are small, the Taylor's series can be truncated, and the functional dependency on these changes thus becomes linear. In a prism infinitely extended in one direction, with uniform density, and with cross sectional shape defined by an N-sided polygon, if A_i represent one of L discrete measurements of gravity anomaly, we would have:

$$A_i = A(x'_1, z'_1, x'_2, z'_2, \ldots, x'_N, z'_N, x_i, z_i) = A(x_i, z_i, w) \quad i = 1, 2, \ldots, L \tag{1}$$

where (x_i, z_i) is the location of the i[th] measurement, the primed coordinates are the N corners of the polygon, represented in shorthand by the 2N-dimentional array, w includes only the body coordinates. For the sake of discussion, let A_i and $\overline{A_\iota}$ represent the observed and calculated anomalies, respectively, at one observation point. We define cost function E as below:

$$E^2 = \sum_{i=1}^{L}[A_i - \overline{A_\iota}(w)]^2 \tag{2}$$

$\overline{A_\iota}$ is a nonlinear function of w, $\overline{A_\iota}$ will be nearly a linear function of those changes. Let $w^{(k)}$ represent the values of $(x'_1, z'_1, x'_2, z'_2, \ldots, x'_N, z'_N)$ after the k the iteration. Then the Taylor's series expansion of the anomaly at point i is:

$$\overline{A_\iota}(w^{(k+1)}) \approx \overline{A_\iota}(w^{(k)}) + \sum_{m=1}^{2N}\frac{\delta}{\delta w_m}\overline{A_\iota}(w^{(k)})\Delta w_m^{(k)} \quad i = 1, 2, \ldots, L \tag{3}$$

where $\Delta w_m^{(k)} = w_m^{(k+1)} - w_m^{(k)}$, m= 1, 2, …, 2N, now substitute equation 3 into equation 2 to get:

$$E^2 = \sum_{i=1}^{L}[A_i - \overline{A_\iota}(w^k) - \sum_{m=1}^{2N}\frac{\delta}{\delta w_m}\overline{A_\iota}(w^{(k)})\Delta w_m^{(k)}]^2 \tag{4}$$

To find the parameters that provide the smallest E^2, we calculate the partial derivative of E^2 $with$ respect to w_j, j= 1, 2, …, 2N, and set each equation equal to zero:

$$\sum_{i=1}^{L}[A_i - \overline{A_\iota}(w^k) - \sum_{m=1}^{2N}\frac{\delta}{\delta w_m}\overline{A_\iota}(w^{(k)})\Delta w_m^{(k)}].[\frac{\delta}{\delta w_j}\overline{A_\iota}(w^{(k)})]=0 \quad j = 1, 2, \ldots, 2N \tag{5}$$

Where we have dropped higher-order terms:

$$\alpha_j = \sum_{m=1}^{2N} G_{mj}\Delta w_m^{(k)} \tag{6}$$

Following the algorithm of Marquardt, equation 6 becomes:

$$\alpha_j = \sum_{m=1}^{M} G_{mj}\Delta w_m^{(k)}(1+\delta_{mj}\boldsymbol{\lambda}) \tag{7}$$

Where:

$$\delta_{mj} = \begin{cases} 0 & if \quad m \neq j \\ 1 & if \quad m = j \end{cases}$$

If $\boldsymbol{\lambda}$=0 equation 7 reduces to equation 6 for $\boldsymbol{\lambda}$>0 the new values of $w^{(k+1)}$are restricted to a neighborhood about $w^{(k)}$; as $\boldsymbol{\lambda}\to\infty$, Equation 7 becomes the method of steepest descend.

The classical least squares solution Z_s is given by the formula (Morrison 1969):

$$Z_s = H_s y \tag{8}$$

With

$$H_s = (A^T A)^{-1}A^T \tag{9}$$

The least squares inverse H_s is formed under the assumption that N>M, i.e. the linear system is over constrained. Likewise, it is required that the rank of A is equal to M, otherwise we could not evaluate$(A^T A)^{-1}$ of (9).

The properties of H_s can be explored by applying the decomposition theorem.

$$A = U\,\Lambda\,V^T \tag{10}$$

where Λ is a M X M diagonal matrix with the eigenvalues $\lambda_1, \ldots, \lambda_M$ along the diagonal. Matrices U and V are constructed from columns of the eigen vectors $U_n$andV_n, respectively of the eigenvalue equations:

$$AA^T U_j = \lambda_j^2 U_j \quad j = I, N \tag{11}$$

$$A^T A\,V_j = \lambda_j^2 V_j \quad j = I, M \tag{12}$$

The eigenvalues λ_j are conveniently arranged in decreasing order, so that $\lambda_1 > \lambda_2 > \lambda_3 \ldots > \lambda_M$. In least square problems the rank of A is assumed to be equal to M, and the surplus eigen values of equation (11)$\lambda_{M+1}, \lambda_{M+2}, \ldots, \lambda_N$ are equal to zero.

U and V are unitary matrices of rank N and M, respectively. Inserting (10) into (9) gives

$$H_s = (V\Lambda U^T\,U\Lambda\,V^T)^{-1}\,U\Lambda\,V^T = V\Lambda^{-1}U^T \tag{13}$$

We now re-parameterize our inverse equation (8) by introducing a new generalized model vector $\zeta = V^T Z$.

Equation (8) then reads [12]:

$$(\zeta_1 \ldots \zeta_M) = \zeta = \Lambda_\eta^{-1} = \begin{Bmatrix} I/\lambda_1 & \ldots & 0 \\ \vdots & & \vdots \\ 0 & \ldots & I/\lambda_M \end{Bmatrix}\begin{Bmatrix}\eta_1 \\ \vdots \\ \eta\end{Bmatrix}. \tag{14}$$

4. Modeling the Lavarestan anticline

The complete Bouger gravity map of Lavarestan was used for 2D modelling. Figure 2 shows the location of the profiles which are used for gravity modeling.

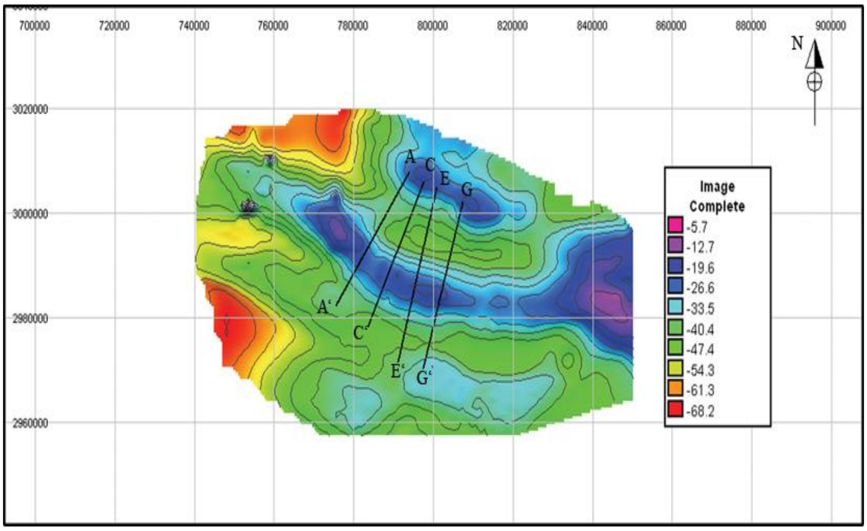

Figure 2. Complete Bouger view of Lavarstan anticline and position of profiles (contour interval is 4 mGal, WGS 84, UTM 40N).

2D modeling was performed on 4 profiles namely: AA', CC', EE' and GG which are composed of 50 point and their length and azimuth is respectively as (31024.14, 215.31), (31135.12, 206.57), (34170.7, 196.87), (33893.44, 197.76).

NIOC based on local evidences, geological measurements and rock sampling was prepared Structural geology section of EE' profile. This section was used as primary model for 2D gravity modeling of mentioned profile. In addition to potential (gravity and magnetic) measurements in coastal Fars project, rock sampling operation was performed to define density of major formations of study area by using laboratory studies [2]. By taking into account the similarities in material and range of rock densities, seven layers were selected and categorized based on density obtained from rock sampling operation and well logs of adjacent structures. Table 1 presents the properties of stratum which used in the model.

Table 1. The properties of stratum which used in the model.

Stratum	Density (in surface)	Density (using logs)	Density variance in model
Aghajari	2.03	...	2.03-2.26
Mishan	2.12	...	
Gurilimeston	...	...	
Gachsaran	2.19	...	
Asmari	2.52	...	2.27-2.52
Pabdeh	...	...	
Gurpi	2.36	...	2.21-2.46
Bangestan	...	...	
Khami	2.29	...	
Kazerun	...	3.42	3.37-3.46
Dehram	...	3.19	2.77-3.19
Lower Paleozoic	...	...	2.72-3.7
Hormoz salt	1.92	...	1.92-2.6

Each layer is defined by different node, during the 2D gravity modeling procedures geometry of nodes interactively varied until the difference of the modeled and observed data become minimized. Figure 3 presents a sample of discussed gravimetric modeling of EE' profile. In part A (Figure 3), the first, second and third layers were included in the model. The modeling procedure continues until suitable correlation was achieved between observed and modeled data. In the next stage, Kazerun and Dehram groups were added into the model and in part C two last layers were added into the model.

Modeling procedure was the same for all the profiles. Underground contours of Kazerun and top of Lower Paleozoic were plotted based on the depth extracted from results of 2D Gravity modeling due to whole profiles (AA' to GG'). In Figures 4 and 5, the map of underground contours maps (ugc) of Kangan and Lower paleozoic structures were obtained from gravimetric modeling is presented.

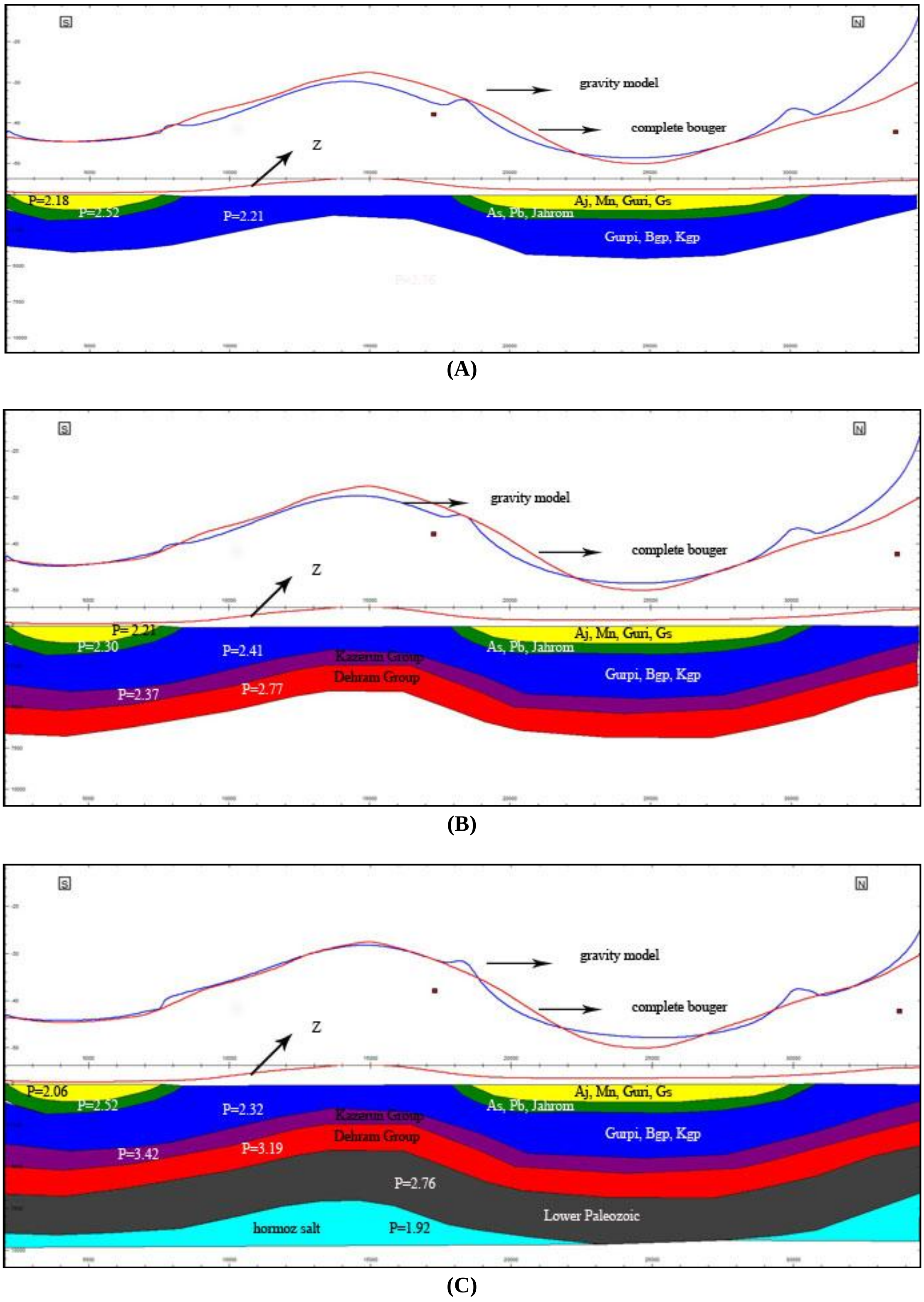

Figure 3. 2D gravity model generated for EE' profile, in part A,B and C different layers have been added in to the model, the blue curve indicates gravity model data and red one shows observed data.

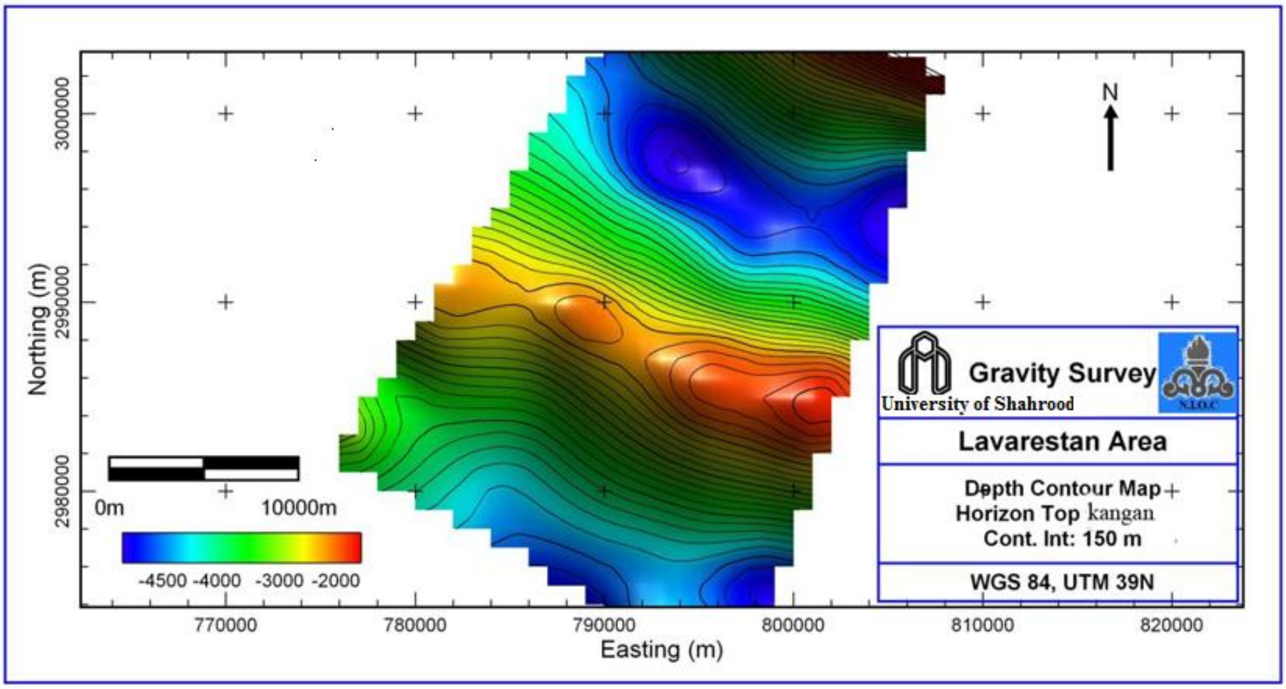

Figure 4. Underground contours map of horizon top of Kangan (obtained from 2D gravimetric modeling).

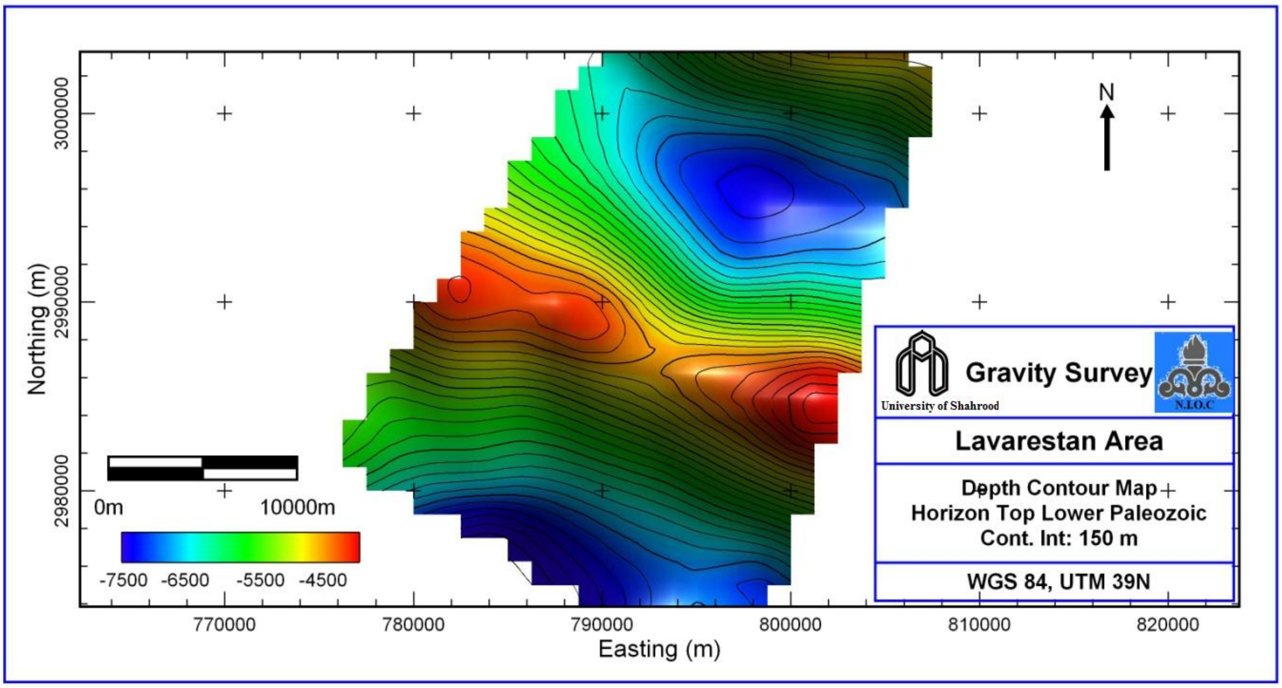

Figure 5. Underground contours map of horizon top of Lower Paleozoic (obtained from 2D gravimetric modeling).

Figure 6 presents these structures together with the topography of location in two views. In 2010 a two-dimensional seismic survey was performed in study area. The result of seismic interpretation on line "Lav03" (shows in Figure 7), confirmed the result of 2D gravity modeling [8]. As mentioned before, Figure 4 (extracted from 2D gravity modeling) shows the top of anticline in Kangan formation about 2000m below the earth surface. Seismic interpretation result on line "Lav03" shows the top of Kangan formation about 2040m below the surface. With respect to this point that the EE' profile is closely to seismic line (Lav03), there is a desire correlation between results from potential field modeling and 2D seismic interpretation.

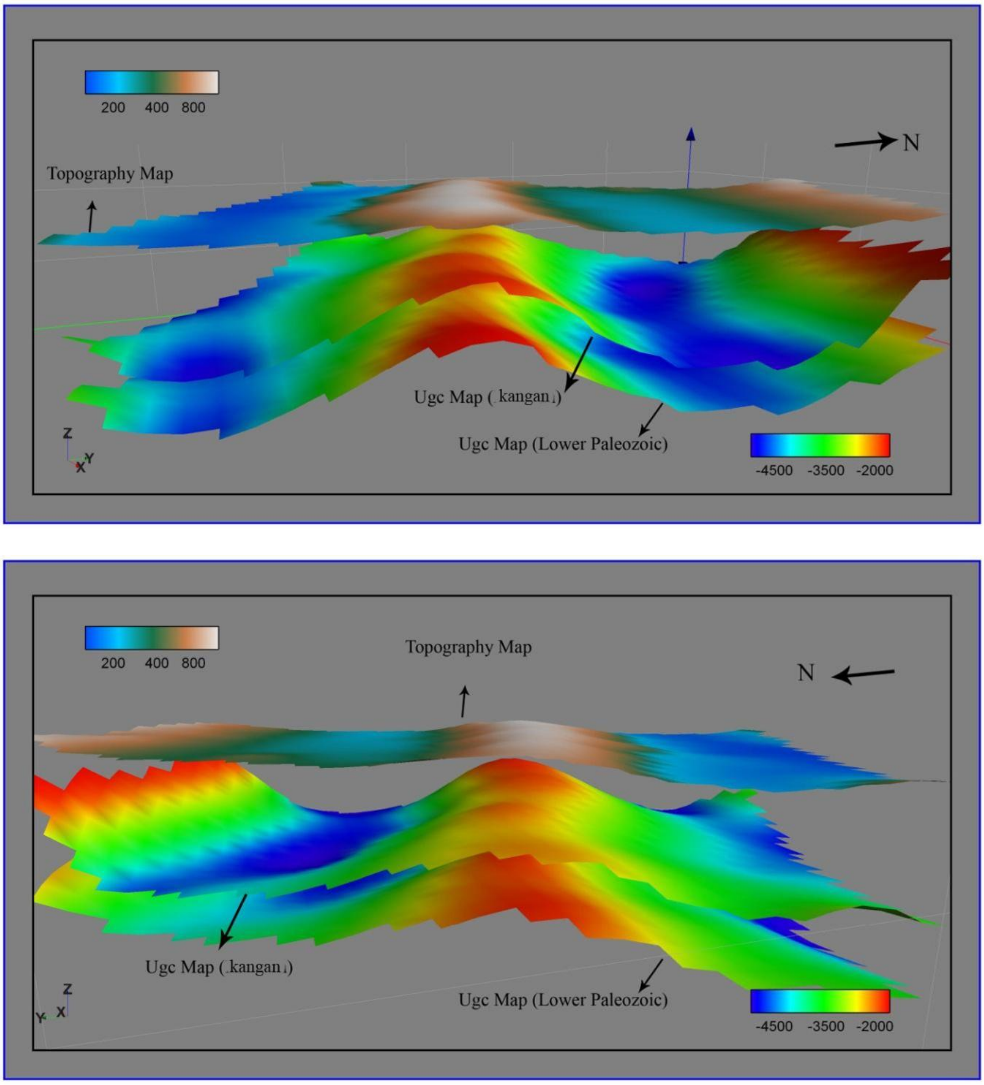

Figure 6. 3D schematic view of Kangan and lower Paleozoic with topography map in two view (Y axis is north direction).

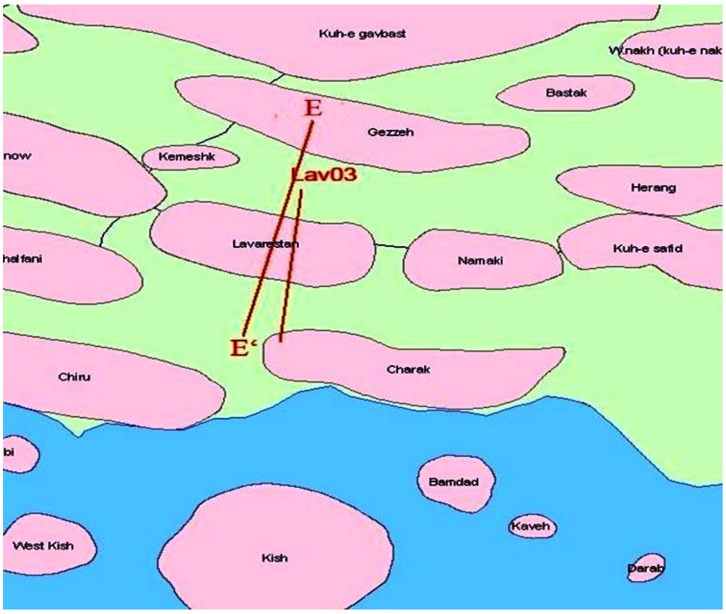

Figure 7. Location of EE' profile and Lav03 seismic line in study area.

5. Conclusions

Geophysical potential field data, specially gravity data, are of great importance in the optimization of underground simulations. 2D Gravity data modeling can present significant information about geological structures. The confidence on the results of 2D Gravity data modeling increases when additional information like rock sampling, well log data and structural geology were involved on modeling. Generally UGC map are extracted from seismic data after interpretation. The location of future well log and expansion program for oil/gas filed are strongly effected by UGC maps. In this paper, the UGC map of Lower Paleozoic and Kazerun are extracted from 2D Gravity modeling with prior information. The result show an appropriate correlation between UGC map of Gravity data and interpretation seismic data. Acquisition and interpretation of the gravity data have lower cast compared to acquiring seismic data. So this agreement between the two type of UGC map can be used for cast optimization in the exploration program for oil/gas fields.

Acknowledgments

The authors would like to thank the National Iranian Oil Company (NIOC) for providing data and ModelVision Pro and PA software.

References

[1]. Akbar Hoseini, A., Doulati Ardejani, F., Tabatabaie, H. and Hezarkhani, A. (2014). A tree-dimensional multi-body inversion process of gravity fields of Gheshm sedimentary basin, Arab J Sci Eng 39: 5603-5611.

[2]. Lowrie, W. (1997). Fundamentals of geophysics. Cambridge university press.

[3]. Hinze, W.J. (1991). The role of gravity and magnetic methods in engineering and environmental studies. In: Ward (ed.) Geotechnical and Environmental Geophysics. The society of exploration geophysics. 75-126.

[4]. Jenkins, A. J. O., Messfin, D. and Moon, W. (1983). Gravity modelling of salt domes and pinnacle reefs. J. Can. Soc. Explor. Geophys. 19 (1): 51–56.

[5]. Talwani, M. (2011). Non linear inversion of gravity gradients and the GGI gradiometer. Central Eur. J. Geosci. 3 (4): 424-434.

[6]. Oruc, B. (2011). Edge detection and depth estimation using a Tilt angle map from gravity gradient data of the Kozakl-Central Anatolia region, Turkey. Pure Appl. Geophys. 168: 1769-1780.

[7]. Barnes, G. and Barraud, J. (2012). Imaging geologic surfaces by inverting gravity gradient data with depth horizons. Geophysics. 77 (1): 1–11

[8]. National Iranian Oil Company. (2004). Interpretation report of coastal fars G/M data. Non-Seismic group, Geophysical Department.

[9]. Encom Technology pty Ltd. (2003). Modelvision Pro Microsoft, The 3D workbench for magnetic and gravity interpretation, Version 10.

[10]. Motamedi, H. and Tahmasebi Sarvestani, A. (2009). Stratigraphical, structural and sedimentary report of fars area. Surface geology office of Exploration national Iran oil company.

[11]. Seif, H. (2011). Structural study of Lavarestan anticline. Master's thesis, Islamic azad university Tehran branch.

[12]. Borsting Pederson, L. (1977). Interpretation of potential field data- A generalized inverse approach, geophysical prospecting. 25: 199-230.

به نقشه درآوردن کنتورهای زیرسطحی، با استفاده از میدان پتانسیل و نتایج چاه و مقایسه با تفسیر لرزه‌ای در منطقه لاورستان

معصومه فخرراد[۱]، علی نجاتی کلاته[۱*] و شهاب قمی[۲]

۱- دانشکده معدن، نفت و ژئوفیزیک، دانشگاه شاهرود، ایران
۲- شرکت مدیریت اکتشاف نفت، تهران، ایران

ارسال ۲۰۱۳/۹/۱۴، پذیرش ۲۰۱۴/۱۰/۱۹

* نویسنده مسئول مکاتبات: nejati@shahroodut.ac.ir

چکیده:

پروژه گرانی‌سنجی فارس ساحلی در محدوده فارس برای پیدا کردن گنبدهای نمکی مدفون و برای تعیین ویژگی‌های گسل‌ها در منطقه انجام شد. ساختمان لاورستان به‌وسیله ۴۲۰۳ ایستگاه گرانی‌سنجی در یک شبکه منظم ۲۵۰×۱۰۰۰ متر پوشش داده‌شده است. در مطالعات قبلی، مدل عمقی ساختمانی از این تاقدیس بر پایه اطلاعات زمین‌شناختی و اندازه‌گیری‌های ساختاری زمین‌شناسی تهیه شده بود. برای داشتن یک پوشش کامل روی این تاقدیس، چهار پروفیل با فاصله مناسب بر روی داده‌های میدان پتانسیل و به‌منظور پردازش و تفسیر بیشتر انتخاب شد. با استفاده از نرم‌افزارهای Encome PA و Encome Modelvision مدل‌سازی معکوس دوبعدی روی این پروفیل‌ها انجام شد. پارامترهای فیزیکی و هندسی برای هر لایه قدم‌به‌قدم تغییر داده شد و محاسبات مدل مستقیم میدان پتانسیل تا به دست آوردن تطابق مناسب بین آنومالی محاسبه‌شده و آنومالی مشاهده‌شده تکرار شد. نتایج این مدل‌سازی بر روی افق بالایی پالئوزوئیک و کازرون (سنگ پوشش) تمرکز داشته است، همچنین نقشه کنتوری زیرسطحی از داده‌های لرزه‌ای پس از تفسیر استخراج‌شده است. بین نقشه کنتورهای زیرسطحی که از مدل‌سازی به‌دست‌آمده و داده‌های لرزه‌ای تفسیر شده، انطباق مناسبی مشاهده شد.

کلمات کلیدی: مدل‌سازی معکوس، داده‌های میدان پتانسیل، نقشه کنتوری زیرسطحی، Encome Modelvision، لاورستان.